Experimental Evidence for the Existence of the HO_2-H_2O Complex

Simone Aloisio and Joseph S. Francisco*

Departments of Chemistry and Earth and Atmospheric Sciences, Purdue University, West Lafayette, Indiana 47906-1393

Randall R. Friedl*

Jet Propulsion Laboratory, California Institute of Technology, Pasadena, California 91109

Received: February 17, 2000; In Final Form: May 15, 2000

Complex formation in the interaction of HO_2 with H_2O was studied using Fourier transform infrared absorption spectroscopy. Studies were carried out between 230 and 298 K in the presence of excess H_2O. On the basis of measurements of HO_2 disappearance, equilibrium constants (K_c) for the formation of the complex were determined to be 1.7×10^{-16}, 4.1×10^{-17}, and $\leq 4 \times 10^{-18}$ cm^3 molecule^{-1} at 230, 250, and 298 K, respectively. The enthalpy for the reaction forming the complex was determined to be -36 ± 16 kJ mol^{-1}. This is in good agreement with previous estimates made from kinetic measurements and theoretical calculations.

I. Introduction

The hydroperoxyl self-reaction

$$HO_2 + HO_2 \rightarrow H_2O_2 + O_2 \quad (1)$$

plays an important role in the atmospheric chemistry of odd hydrogen, HO_x, and is the primary source of hydrogen peroxide in the atmosphere.[1] The reaction rate coefficient displays complicated functional behavior, with both pressure-dependent and pressure-independent pathways. This behavior has been rationalized in terms of a complex reaction mechanism involving an H_2O_4 intermediate. Water vapor has been found to enhance the reaction rate coefficient to a larger degree than can be explained by the increased vibrational quenching of H_2O relative to the normal buffer gases N_2 and O_2.[2−10] Lii et al.[7] accounted for the H_2O dependence with a multistep mechanism involving rapid formation of a water-complexed HO_2, i.e., HO_2-H_2O.

$$HO_2 + H_2O \rightleftarrows HO_2-H_2O \quad (2)$$

On the basis of this mechanism, Kircher and Sander[10] have quantified the enhancement with the following expression:

$$k_1 = k_1^\circ \times \{1 + 1.4 \times 10^{-21}[H_2O] \exp(2200/T)\} \quad (3)$$

where k_1° refers to the condition with $[H_2O] = 0$. An enthalpy of formation of -37.6 kJ mol^{-1} for the HO_2-H_2O complex has been deduced from the measured kinetic parameters, assuming the mechanism of Lii et al.[7] This value compares reasonably well with the theoretically calculated values of -31 kJ mol^{-1} and -32 kJ mol^{-1} obtained by Hamilton and Naleway[11] and Aloisio and Francisco,[12] respectively.

At present, there have been no direct experimental observations of the complex in the gas phase from which thermodynamic properties can be deduced. Previous kinetic studies have utilized HO_2 detection methods, such as UV absorption and mass spectrometry, that are likely to be equally sensitive to HO_2-H_2O. Consequently, it was assumed in those experiments that decreases in signal in the presence of H_2O could not be attributed to the conversion of HO_2 to HO_2-H_2O, which would yield no net signal change, but rather to reactions of HO_2-H_2O with itself and with HO_2 that do not conserve the sum of the two species. Recently, the complex has been identified in a solid matrix by Nelander[13] on the basis of observed infrared absorption features at 3236.2 cm^{-1} (ν_1), 1479.3 cm^{-1} (ν_2), and 1120.4 cm^{-1} (ν_3). The matrix data do not allow for an enthalpy of formation to be derived, however.

In this work, we have attempted to obtain direct confirmation of the existence of the complex in the gas phase by probing gaseous mixtures of HO_2 and H_2O with infrared absorption spectroscopy in the 1100−1140 cm^{-1} region. On the basis of the observed depletion of HO_2 in the presence of excess H_2O, as evidenced by decreases in HO_2 rotational line absorptions, we infer formation of the HO_2-H_2O complex. The observed temperature dependence of the HO_2 loss is used to derive the enthalpy of formation of the complex. The derived thermochemical properties enable us to assess the importance of this complex in the Earth's atmosphere.

II. Experimental Methods

The experiment was performed using a discharge flow cell and a Bomem FT-IR spectrometer with multipass optics that has been described previously.[14] A schematic of the instrument, including modifications made for this experiment, is shown in Figure 1. The hydroperoxyl radical was made by reacting fluorine atoms with hydrogen peroxide.

$$F + H_2O_2 \rightarrow HO_2 + HF \quad (4)$$

Fluorine atoms were generated in a reactor sidearm by passage of molecular fluorine through a microwave discharge. The flow of atoms was mixed with a hydrogen peroxide flow, generated by the passage of helium carrier gas through a glass bubbler containing linquid H_2O_2, inside the main reactor portion of the apparatus, approximately 100 cm upstream of the infrared multipass absorption cell. Near stoichiometric conversion of F

10.1021/jp0006330 CCC: $19.00
Published on Web 06/22/2000

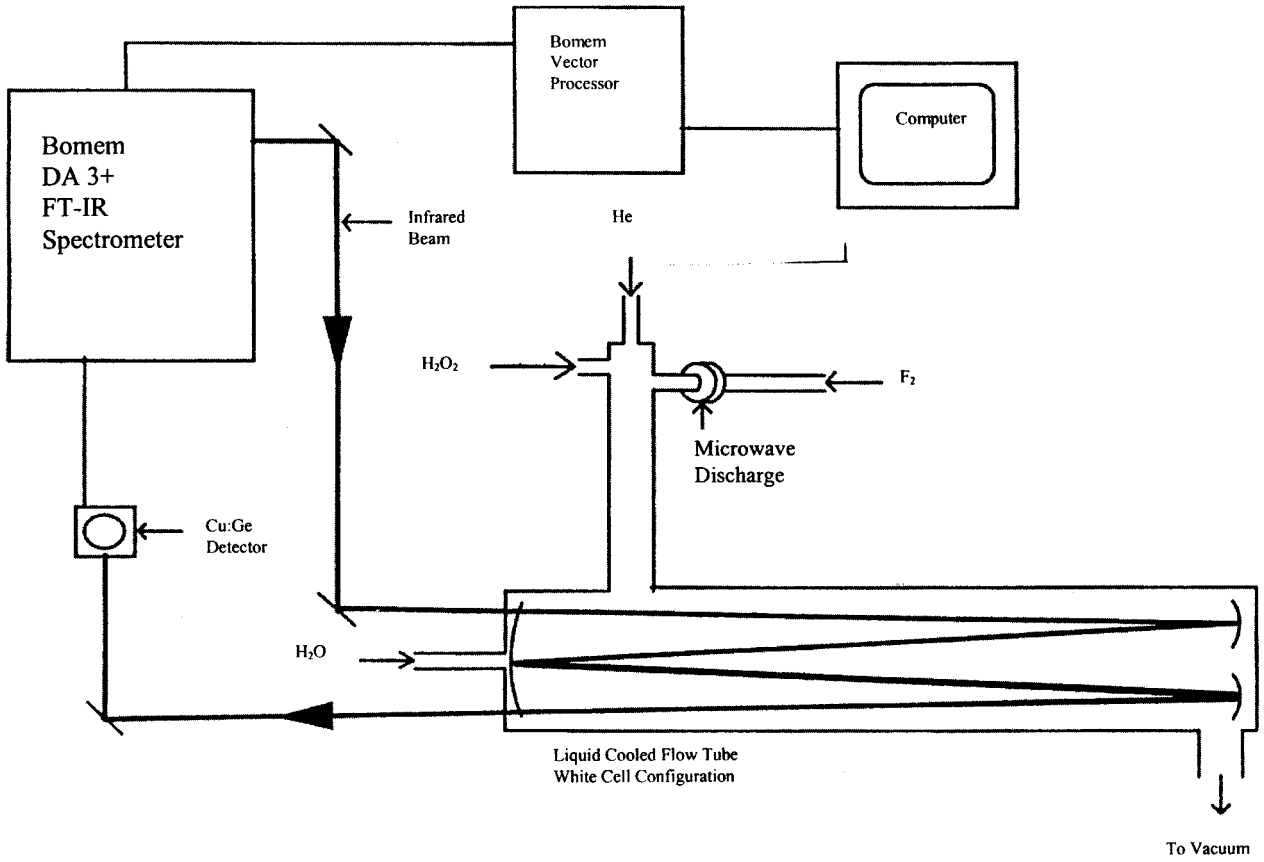

Figure 1. Diagram of the instrument used in these experiments.

to HO_2, prior to entry into the absorption cell, was achieved by maintaining a $[H_2O_2]$ to [F] ratio in excess of 5. Initial HO_2 concentrations of up to 1×10^{14} molecule cm^{-3} in the reactor could be achieved using this chemical titration scheme. Conversion of F to HO_2 was verified by two methods. First, the hydrogen peroxide infrared signal was monitored with and without the discharge and a decrease in H_2O_2 signal was observed with the discharge on. Second, NO was added to the flowtube, and some of it was converted to NO_2, presumably by reaction with the HO_2 being formed.

Formation of the HO_2-H_2O complex was attempted by adding an excess of water vapor, relative to the HO_2 at the upstream end of the absorption cell. Gaseous water vapor concentrations of up to 1×10^{16} molecule cm^{-3} were added in to the absorption cell by passing helium through a glass bubbler filled with liquid water. The total pressure in the absorption cell was maintained at approximately 0.8 Torr by addition of excess helium. Residence times in the absorption cell were decreased to approximately 100 ms in order to minimize loss of HO_2 molecules through the HO_2 self-reaction. In addition, the flow tube was coated with halocarbon wax in order to minimize wall loss of HO_2. Differences in the wall loss rates between HO_2 and the HO_2-H_2O complex are assumed to be small. No wall loss measurements were performed in this study, however. The entire flow system (reactor plus absorption cell) was temperature controlled between 230 and 298 K by cycling liquid-nitrogen-cooled methanol through an outer glass jacket.

Spectroscopic probing of the reactants and products was carried out using a Bomem DA3+.002 Fourier transform spectrometer equipped with a globar infrared source and a KCl beam splitter. Signal was detected using a liquid-helium-cooled copper-doped germanium detector (Santa Barbara Research) equipped with narrow band-pass filters for the regions of interest. The cell was configured with a White-type optics cell that provided a total optical path length of 48 m (32 passes of the 1.5-m flow-tube length). High-resolution (0.04 cm^{-1}, apodized) spectra with noise levels near 0.1% were obtained by coaddition of approximately 1000 scans (6 h total observation time). The choice of resolution represented a compromise between minimization of the spectrum acquisition time and resolution of individual and/or blended HO_2 lines

The gases used in this experiment were obtained from Spectra Gas (F_2, 5% in He) and Airco (He, 99.995%). Hydrogen peroxide, obtained from FMC (70% purity), was purified by distillation to at least 95% purity and stored at approximately 0 °C prior to use. Liquid water samples were distilled and deionized prior to use. The number densities of H_2O_2 and H_2O in the reactor were calculated from measured gaseous partial pressures in the bubblers and carrier gas flow rates through the bubblers. Additionally, H_2O_2 concentrations were estimated using IR and UV absorption data, the former utilizing H_2O_2 rotational line measurements in the 1100 cm^{-1} region and absorption cross sections obtained in past experiments,[15] and the latter using a single pass of deuterium lamp radiation directed through the absorption cell and onto a diode array detector (PARC model 1461/1412 OMA 111, equipped with a 600-groove/mm grating). UV measurements at 250 nm were converted to H_2O_2 concentrations using the NASA-recommended[16] absorption cross sections. The three methods yielded H_2O_2 concentrations that were in good agreement with one another. Concentrations of fluorine atoms in the reactor were estimated from measured gas flow rates and cell pressures under the assumption of complete dissociation of molecular fluorine in the discharge region. Finally, HO_2 concentrations were estimated by assuming stoichiometric conversion of the F atoms.

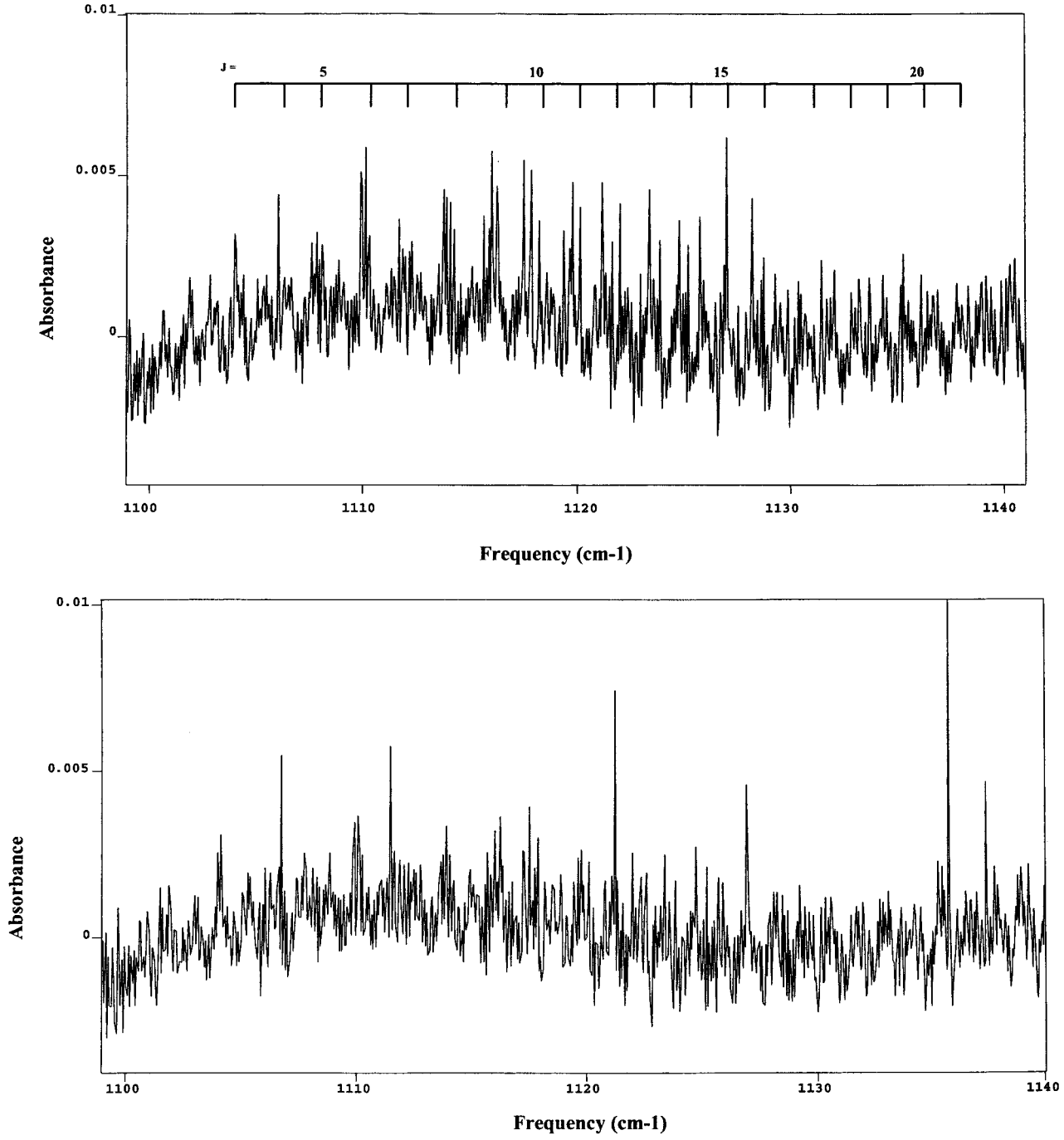

Figure 2. (a) Absorption spectrum of the ν_3 band of HO_2 without water. (b) Absorption spectrum of the ν_3 band of HO_2 with water.

III. Results

The column abundance of HO_2 in the absorption cell was monitored through its ν_3 vibrational band (Figure 2a). This band was preferred to the ν_1 and ν_2 bands, which were also observable, because of the relative lack of interference by H_2O and H_2O_2 bands in the ν_3 spectral region. The ν_3 band has been characterized previously in terms of both rotational line assignments and line strengths.[17] We were able to observe over 70 HO_2 absorption features between 1107 and 1134 cm^{-1}, with signal-to-noise ratios approaching 10:1. The noise level for these spectra are approximately 0.1%. Many of the absorption features were blended lines.

Typical HO_2 peak line absorbances obtained were on the order of 1%, corresponding to column abundances of approximately 5×10^{16} molecule cm^{-2} and average HO_2 concentrations of 3×10^{12} cm^{-3}. Because of the HO_2 self-reaction (reaction 1) an axial gradient was established over the length of the absorption cell. On the basis of the recommended Arrhenius expression for the pressure-independent HO_2 self-reaction rate coefficient, i.e., $k_1^\circ = 2.3 \times 10^{-13}\exp(600/T)$, we calculate that HO_2 concentrations decreased from the upstream to the downstream end of the absorption cell by approximate factors of 4, 6, and 7 at 298, 250, and 230 K, respectively, for initial HO_2 concentrations of 1×10^{14} molecule cm^{-3}.

No discernible decrease in the HO_2 column abundance (<5%) was evident when water vapor was introduced into the absorption cell at room temperature. For these trials, water vapor concentrations were increased to approximately 1.5×10^{16} molecule cm^{-3}, a limit dictated by the cell total pressure constraint. At the lower temperatures investigated, addition of

water vapor resulted in marked decreases in HO_2 column abundances (see Figure 2b). Limitations on the amount of added water vapor became more severe at the lower temperatures because of concern over condensation and possible increased HO_2 wall loss. UV absorption measurements, showing substantial loss of beam transmission at the onset of ice crystal growth, were used to define the maximum water vapor concentrations of 1×10^{16} molecules cm^{-3} at 250 K and 2×10^{15} molecules cm^{-3} at 230 K. For these water vapor concentrations, the associated decreases in HO_2 column abundance were $41 \pm 11\%$ at 250 K and $34 \pm 12\%$ at 230 K as calculated by taking the ratio of the sample and reference spectra for 18 of the strongest HO_2 absorption lines.

The observed HO_2 column decreases are substantially larger than can be explained by the known H_2O-catalyzed rate increase of the HO_2 self-reaction. According to eq 3, the rate constant for reaction 1 under our experimental conditions increases by a factor of 1.09 at 250 K and 1.04 at 230 K. These increases in the HO_2 self-reaction rate translate to decreases in the HO_2 column abundance of only 5% and 3% at 250 and 230 K, respectively. As is evidenced by the data of Kircher and Sander,[10] the uncertainties attached to the parameters in eq 3 are far less than those required to explain our current observations. Consequently, we attribute the differences between observed and expected HO_2 behavior to the formation of a molecular complex between the hydroperoxyl radical and water, i.e., to reaction 2. The observed decreases in the HO_2 spectral lines were accompanied by the appearance of a number of new spectral features in the 1100−1140 cm^{-1} region. The new features suffer from a poor signal-to-noise ratio (2:1) and are not readily assigned.

The enthalpy of reaction 2 can be derived from the experimental HO_2 data provided that equilibrium is established rapidly, i.e., within 10 ms, between HO_2 and the complex. This proviso requires the termolecular rate coefficient for reaction 2 to be greater than 10^{-31} cm^6 $molecule^{-2}$ s^{-1}. Although we cannot verify that equilibrium is established, this is a plausible value given the expected large binding energy and high number of low-frequency vibrations associated with HO_2-H_2O. The equilibrium constant for reaction 2 can be written as

$$K_c = \frac{[HO_2 - H_2O]}{[HO_2][H_2O]} = \frac{\Delta HO_2}{[HO_2][H_2O]} \qquad (5)$$

where the equilibrium constant is given in units of cubic centimeters per molecule and ΔHO_2 is the fractional decrease in the HO_2 column abundance with addition of H_2O. On the basis of the observed HO_2 decreases, we derive equilibrium constants of $(4.1 \pm 1.1) \times 10^{-17}$ cm^3 $molecule^{-1}$ and $(1.7 \pm 0.6) \times 10^{-16}$ cm^3 $molecule^{-1}$ at 250 and 230 K, respectively. From the room-temperature measurements, we infer an upper bound of 4×10^{-18} cm^3 $molecule^{-1}$ for the equilibrium constant at 298 K.

From these data, one can calculate the heat of reaction, ΔH, for reaction 2 using the equation

$$d(\ln K_p) = \frac{\Delta H}{R} d(T^{-1}) \qquad (6)$$

where K_p is the equilibrium constant in terms of pressure, R is the ideal gas constant, and T is the temperature. The relationship between K_p and K_c for bimolecular complexes is treated by Vigasin.[18] By making a van't Hoff plot of $\ln K_p$ vs T^{-1}, ΔH is obtained from the slope of the line and ΔS from the intercept. Using this method, a value of (-36 ± 16) kJ mol^{-1} is obtained for the reaction enthalpy. Similarly, a value of (-85 ± 40) J mol^{-1} K^{-1} is calculated for the reaction entropy. The present results are summarized and compared with previous estimates in Table 1. There is good agreement between the results of this work and those of Cox and Burrows,[5] with the latter being based on experimental kinetics data. Both of the experimentally based estimates yield enthalpies that are approximately 15% higher and entropies that are approximately 20% lower than those derived from previous theoretical treatments. Given the theoretical and experimental difficulties in studying the HO_2-H_2O complex, these differences are not considered to be significant.

TABLE 1: Thermodynamic Data

	this work	ref 11	ref 12
ΔH^a	-36 ± 16	-31	-32
ΔS^b	-85 ± 40	-103	-107

[a] Units for ΔH are kJ mol^{-1}. [b] Units for ΔS are J mol^{-1} K^{-1}.

IV. Discussion

Application of high-resolution infrared spectroscopy to the $HO_2 + H_2O$ system has provided us with a unique diagnostic for decoupling reactive changes in HO_2 and HO_2-H_2O concentrations. Using this probe, we have observed HO_2 loss in the presence of H_2O that cannot be rationalized in terms of the previously characterized H_2O-catalyzed acceleration of the HO_2 self-reaction. An analysis of the data in terms of HO_2-H_2O formation yields enthalpy and entropy values that are consistent with previous estimates determined both theoretically and experimentally. Taken together, the various studies provide strong evidence for the existence of an HO_2-H_2O complex with a binding energy of approximately 35 kJ mol^{-1}.

The relative stability of the complex coupled with the presence of large ambient concentrations of H_2O, implies that HO_2-H_2O may coexist with HO_2 in the Earth's atmosphere. Both the atmospheric water vapor concentration and the reaction 2 equilibrium constant are strong functions of altitude; however, they vary in opposite directions. On one hand, $[H_2O]$ decreases from approximately 3×10^{17} molecule cm^{-3} near the surface to 2×10^{13} molecule cm^{-3} at the tropopause. On the other hand, the equilibrium constant increases from approximately 2×10^{-18} cm^3 $molecule^{-1}$ near the surface to 1×10^{-15} cm^3 $molecule^{-1}$ at the tropopause. Convolution of these parameters favors HO_2-H_2O formation at altitudes between 1 and 3 km. In that altitude range, HO_2-H_2O levels may rise to 30% of HO_2 levels.

Because of its fast chemical coupling with HO_2 through reaction 2, the primary atmospheric role of HO_2-H_2O is as a temporary reservoir of HO_2. A number of chemical and photochemical processes involving HO_2-H_2O carry the potential to affect atmospheric HO_x levels, namely

$$HO_2-H_2O + HO_2 \rightarrow H_2O_2 + H_2O + O_2 \qquad (7)$$

$$HO_2-H_2O + HO_2-H_2O \rightarrow H_2O_2 + O_2 + 2H_2 \qquad (8)$$

$$HO_2-H_2O + h\nu \rightarrow \text{products} \qquad (9)$$

$$HO_2-H_2O + \text{aerosol/cloud} \rightarrow H_2O_2 + \text{other condensed products} \qquad (10)$$

Reactions 7 and 8 are likely to be faster than the HO_2 self-reaction (reaction 1) but are presumably captured in the kinetic results that form the basis of the NASA[16] recommendations for reaction 1. Reactions 9 and 10 are unlikely to be substantially faster than the analogous HO_2 processes. In the case of reaction 9, no distinct spectral features, apart from those already known for HO_2, have been observed under conditions where HO_2 and

HO_2-H_2O should coexist. This implies that neither the absorption spectrum nor the cross sections of HO_2-H_2O are significantly different than those of HO_2. In the case of reaction 10, although there are no data on HO_2-H_2O heterogeneous chemistry, previous studies have shown that HO_2 is taken up with near unit probability by a number of different surface types.[16] It is also possible that complexation affects the wall loss rate of HO_2 in experiments. As mentioned earlier however, we have no evidence to indicating this was the case.

Acknowledgment. The authors thank Jurgen Linke for his master craftsmanship in glasswork, which he made readily available to us many times through the duration of this work. We also thank Dr. Kyle Bayes, Dr. Barna Laszlo and Dr. Francois Caloz for their indispensable suggestions. The research described in this paper was partly carried out at the Jet Propulsion Laboratory, California Institute of Technology, under contract with the National Aeronautics and Space Administration. S. Aloisio was a visiting scientist at the Jet Propulsion Lab, and he thanks the JPL Chemical Kinetics Group for providing the facilities and instrumentation that made this work possible.

References and Notes

(1) Finlayson-Pitts, B. J.; Pitts, J. N., Jr. *Atmospheric Chemistry*; Wiley: New York, 1986.

(2) Hamilton, E. J., Jr. *J. Chem. Phys.* **1975**, *63*, 3682.

(3) Hochanadel, C. J.; Ghormley, J. A.; Orgen, P. J. *J. Chem. Phys* **1972**, *56*, 4426.

(4) Hamilton, E. J., Jr.; Lii, R.-R. *Int. J. Chem. Kinet.* **1977**, *9*, 875.

(5) Cox, R. A.; Burrows, J. P. *J. Phys. Chem.* **1979**, *83*, 2560.

(6) DeMoore, W. B. *J. Phys. Chem.* **1979**, *83*, 1113.

(7) Lii, R.-R.; Sauer, M. C.; Gordon, S. *J. Phys. Chem.* **1981**, *85*, 2833.

(8) Sander, S. P.; Peterson, M.; Watson, R. T. Patrick, R. *J. Phys. Chem.* **1982**, *86*, 1236.

(9) Andersson, B. Y.; Cox, R. A.; Jenkin, M. E. *Int. J. Chem. Kinet.* **1989**, *20*, 283.

(10) Kircher, C. C.; Sander, S. P. *J. Phys. Chem* **1984**, *88*, 2082.

(11) Hamilton, E. J., Jr.; Naleway, C. A. *J. Phys. Chem* **1976**, *80*, 2037.

(12) Aloisio, S.; Francisco, J. S. *J. Phys. Chem* **1998**, *102*, 1899.

(13) Nelander, B. *J. Phys. Chem.* **1997**, *101*, 9092.

(14) Friedl, R. R.; Sander, S. P. *J. Phys. Chem.* **1987**, *91*, 2721.

(15) Bayes, K. Jet Propulsion Laboratory, Personal communication.

(16) DeMore, W. B.; Sander, S. P.; Golden, D. M.; Hampson, R. F.; Kurylo, M. J.; Howard, C. J.; Ravishankara, A. R.; Kolb, C. E.; Molina, M. J.; *Chemical Kinetics and Photochemical Data for Use in Stratospheric Modeling*; JPL Publication 97-4; NASA: Washington, D.C., 1997.

(17) Burkholder, J. B.; Hammer, P. D.; Howard, C. J. *J. Mol. Spec.* **1992**, *151*, 483.

(18) Vigasin, A. A.; Slanina, Z. *Molecular Complexes in Earth's, Planetary, Cometary and Interstellar Atmospheres*; World Scientific: Singapore, 1998; p 3.